Electrical Power and Energy Systems xxx (2014) xxx–xxx

Contents lists available at ScienceDirect

Electrical Power and Energy Systems

journal homepage: www.elsevier.com/locate/ijepes

# Detailed study of DFIG-based wind turbines to overcome the most severe grid faults

Alejandro Rolán[a], Joaquín Pedra[b], Felipe Córcoles[b,*]

[a] Department of Electrical Engineering, ETSEIAT-UPC, Colom St. 1, Terrassa-Barcelona 08222, Spain
[b] Department of Electrical Engineering, ETSEIB-UPC, Diagonal Av. 647, Barcelona 08028, Spain

ARTICLE INFO

*Article history:*
Received 13 April 2013
Received in revised form 19 April 2014
Accepted 12 May 2014
Available online xxxx

*Keywords:*
Doubly-fed induction generator (DFIG)
Fault clearing
Fault ride-through capability
Rotor-side converter
Symmetrical voltage sag
Unsymmetrical voltage sag

ABSTRACT

This paper studies the effects of voltage sags caused by faults on doubly-fed induction generators to overcome grid faults. A wide range of sag duration and depth values is considered. It is observed that sag duration influence is periodical. Sag effects depend on duration and depth and on the fault-clearing process as well. Two approaches of the model are compared: the most accurate approach, *discrete sag*, considers that the fault is cleared in the successive natural fault-current zeros of affected phases, leading to a voltage recovery in several steps; the least accurate approach, *abrupt sag*, considers that the fault is cleared instantaneously in all affected phases, leading to a one-step voltage recovery. Comparison between both sag models reveals that the fault-clearing process smoothes sag effects. The study assumes that the rotor-side converter can keep constant the transformed rotor current in the synchronous reference frame, thus providing insights into wind turbine fault ride-through capability. The voltage limit of the rotor-side converter is considered to show the situations where the rotor current can be controlled. Finally, a table and a 3D figure summarizing the effects of the most severe grid faults on the rotor-side converter to overcome the most severe faults are provided.



## Introduction

According to current transmission system operator grid codes, modern wind turbines (WTs) must achieve fault ride-through capability (i.e., they must not disconnect from the grid when a sag occurs, ensuring electricity supply continuity [1]), and they also must contribute to the system stability during and after the fault clearance by means of the active and reactive current during and after the event.

Doubly-fed induction generator (DFIG)-based WT is the most common concept for WT energy systems [2]. This concept has a high susceptibility to voltage sags. Most studies on DFIGs exposed to sags deal with their control under such disturbances. However, few papers concern the most severe grid fault conditions that can damage the rotor-side converter ([3,4] are examples for symmetrical and unsymmetrical sag events, respectively).

In [5], the authors developed an analytical model for DFIGs exposed to sags. In this model, the rotor-side converter is protected against large over currents caused by sags by a simple control strategy: the rotor current in the synchronous reference frame is kept constant at its pre-fault steady-state value during the entire transient. This control strategy also maintains DFIG controllability as established in current grid codes (i.e. not only to stay connected during the fault, but also draw active and reactive current during and after the fault). As the model is analytical, it allowed a large number of scenarios to be easily studied. The voltage limit of the rotor-side converter was also contemplated in the study.

The present paper is a continuation of the above work. DFIGs under voltage sags are exhaustively studied by considering a wide range of sag duration and depth values, and the situations where the rotor current can be controlled are analyzed. The impact of voltage recovery on DFIGs is also investigated. It is observed that sag effects are smoothed when sags are modeled discrete (sags modeled with a voltage recovery in several steps). The simulations are carried out with Matlab. The results provide insights into the fault ride-through capability of DFIG-based WT in order to overcome the most severe grid faults, whose effects are summarized in a table and a 3D figure.

## Voltage sag modeling

In this paper, voltage sags are characterized by duration ($\Delta t$), depth ($h$), fault current angle ($\psi$), typology and fault-clearing

* Corresponding author. Tel.: +34 93 4015890; fax: +34 93 4017433.
*E-mail addresses:* alejandro.rolan@upc.edu (A. Rolán), pedra@ee.upc.edu (J. Pedra), corcoles@ee.upc.edu (F. Córcoles).

http://dx.doi.org/10.1016/j.ijepes.2014.05.031
0142-0615/

process modeling [6,7]. Note that the sag depth ($h$) for the symmetrical sags is the remaining voltage with respect to the pre-fault (nominal) voltage. The sag depth in the unsymmetrical sags is defined by a simple voltage divider on the sequence circuits in radial feeders, as detailed in [6].

According to [7] grid faults can be fully cleared in different ways. All the possibilities are classified into fourteen cases, denoted as $A_1$, $A_2$, $A_3$, $A_4$, $A_5$, B, C, D, $E_1$, $E_2$, $F_1$, $F_2$, $G_1$ and $G_2$. As DFIG stator windings are isolated wye or delta connected, the grid zero-sequence voltage has no influence on DIFG behavior. Consequently, this paper only contemplates the following voltage sags: $A_1$, $A_2$, $A_4$, $A_5$, C, D, $F_1$, $F_2$, $G_1$ and $G_2$, which are shown in Table 1.

As faults are cleared by the circuit breaker in the natural fault-current zeros, unsymmetrical faults involving two fault currents (i.e., 1-phase-to-ground or 2-phase faults) are cleared instantaneously (or abruptly) in all affected phases. This is the case of sag types C and D, which can be indistinctly modeled as abrupt or discrete sags.

In contrast, symmetrical or unsymmetrical faults involving three fault currents (i.e., 3-phase faults, 3-phase-to-ground faults or 2-phase-to-ground faults) are cleared in two or three steps, leading to a discrete voltage recovery. Furthermore, these faults can be fully cleared in different ways, resulting in four discrete symmetrical sag types ($A_1$, $A_2$, $A_4$ and $A_5$) and four discrete unsymmetrical sag types ($F_1$, $F_2$, $G_1$ and $G_2$).

Table 1 also shows the evolution of the events during voltage recovery according to [7]. For example, a sag of type $A_4$ is an event composed of a sag $A_a$ (symmetrical with respect to phase a) during the fault, which evolves into a sag $F_{2a}$ (symmetrical with respect to phase a) after the first voltage recovery, and later into a sag $C_b^*$ (symmetrical with respect to phase b) after the second voltage recovery. Note that faults caused by sags C and D are cleared in one step, as said previously.

## DFIG-based WT characteristics

The chosen 2 MW DFIG-based WT is described in [5]. The following three WT operating points are studied ($s$ being the mechanical slip):

(1) Point 1: rated power and $s = -0.27$.
(2) Point 2: 0.5 times the rated power and $s = -0.09$.
(3) Point 3: 0.1 times the rated power and $s = 0.33$.

## DFIG exposed to voltage sags

### DFIG dynamic equations

The DFIG dynamic equations written in transformed variables, using the *Ku* transformation [8] and considering the motor sign conversion, are

$$\begin{aligned} v_{sf} &= [R_s + L_s(p + j\omega_s)]i_{sf} + M(p + j\omega_s)i_{rf} \\ v_{rf} &= [R_r + L_r(p + js\omega_s)]i_{rf} + M(p + js\omega_s)i_{sf} \\ T_m &= 2\wp M \mathrm{Im}(i_{sf} i_{rf}^*) \quad s = (\omega_s - \wp\omega_m)/\omega_s, \end{aligned} \tag{1}$$

where subscripts s and r stand for the stator and the rotor, subscript f stands for the *forward* component of the transformed variable, is the number of pole pairs, $p$ is the time differential operator d/dt, $T_m$ is the electromagnetic torque, $s$ is the mechanical slip, $\omega_m$ is the generator speed and $\omega_s = 2\pi f_s$ is the pulsation of the stator voltages ($f_s$ is the frequency of the stator voltages, and $T = 1/f_s$ is the period). Note that all rotor magnitudes in (1) are referred to the stator.

### DFIG control strategies during voltage sags

The DFIG behavior during a voltage sag is influenced by two main topics. On the one hand, large rotor currents which cannot be tolerated by the rotor converter are produced during and after the event [9]. On the other hand, current grid codes require to the DFIG to remain connected to the grid, with specific control of the active and reactive currents during and after the fault [3]. Three philosophies can be adopted for the DFIG strategy design:

(1) To disconnect the wind turbine from the grid.
(2) To use a crowbar: a set of resistors short-circuits the machine's rotor. The DFIG remains connected to the grid but it cannot be controlled, as its rotor is short-circuited.
(3) To ensure electricity supply continuity by means of a control strategy in the rotor converter: the DFIG remains connected to the grid and the rotor converter keeps working. However, the philosophy of control during the sag is not a trivial topic and there are very different strategies that can be adopted, depending on the goal to be achieved ([10] compares different control strategies, while [11,12] detail refined control philosophies). The control strategies can be summarized into two types:
   – To reduce the rotor current: it can be suppressed during the sag [13] (thus it has the same problem as the crowbar), or it can be reduced up to a certain value [14]. Another option would be to maintain the pre-event rotor current, as in [15,16].
   – To reduce the rotor voltage [17,18]: in this case it is possible to reduce or damp the stator and the rotor fluxes.

The main problem when using a control strategy is the appearance of large rotor voltage peaks (when controlling the rotor current) or large rotor current peaks (when controlling the rotor voltage) that appear after voltage recovery (see Section 'Comments about the proposed control strategy' for more details). However, these peaks are smoothed when considering the discrete model for the sag. This is an interesting topic, as there are no studies in the literature regarding DFIG-based WTs under voltage sags considering the fault-clearing process.

I should also be noted that the different control strategies result in different DFIG behaviors, with their own strengths and weaknesses. Thus, the use of one or another control philosophy depends on the goal to be achieved. In the present paper it is assumed that the transformed rotor current is kept constant in the synchronous reference frame in order to protect the rotor-side converter from the large rotor current peaks.

### Proposed current control strategy

To study DFIG behavior under voltage sags, the next two assumptions are made:

(1) The rotor-side converter can keep constant the rotor current in the synchronous reference frame, $i_{rf}$, at its pre-fault steady-state value. Moreover, the control is assumed ideal, which means that the controlled variable is adjusted instantaneously to satisfy the set point requirement, i.e., $i_{rf}$ is kept constant throughout the event. It should be noted that the current control loop bandwidth has, in practice, a finite value. However, the authors have considered an ideal control as the first approximation to study the problem. This approach could be considered an idealization of the control strategy used in [15,16], where an hybrid current controller is proposed: the standard PI current controller for non-



Please cite this article in press as: Rolán A et al. Detailed study of DFIG-based wind turbines to overcome the most severe grid faults. Int J Electr Power Energ Syst (2014), http://dx.doi.org/10.1016/j.ijepes.2014.05.031

**Table 1**
Classification of the three-phase voltages at the equipment terminals: sag during the fault and evolution of the sag during the voltage recovery (adapted from [7]). No zero-sequence voltage is considered.

| Evolution of the event | Evolution of the event |
|---|---|
| Type $A_1$ 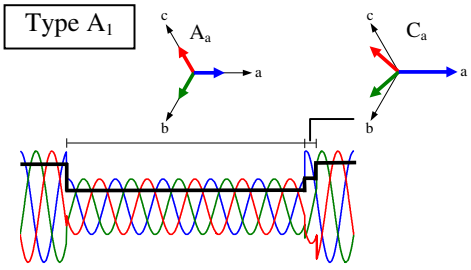 | Type D 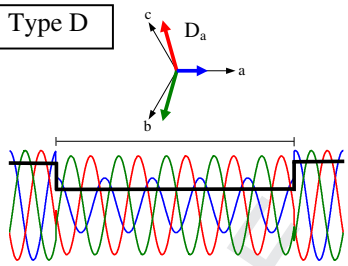 |
| Type $A_2$ 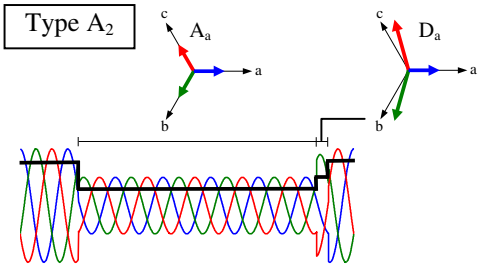 | Type $F_1$ 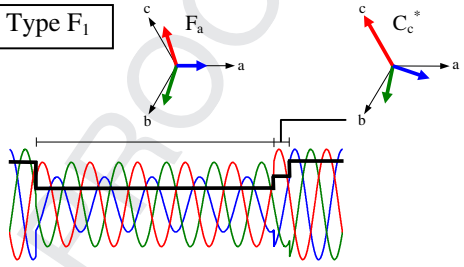 |
| Type $A_4$ 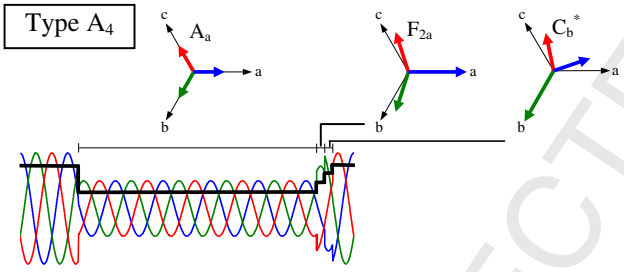 | Type $F_2$ 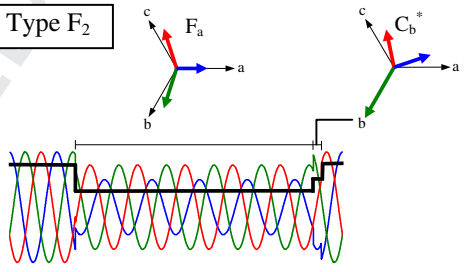 |
| Type $A_5$ 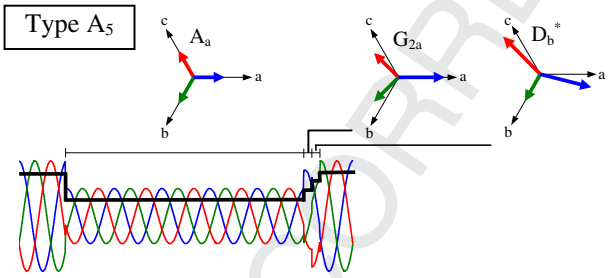 | Type $G_1$ 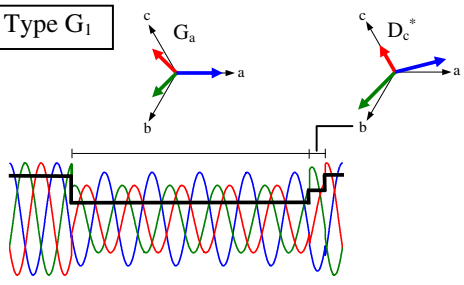 |
| Type C 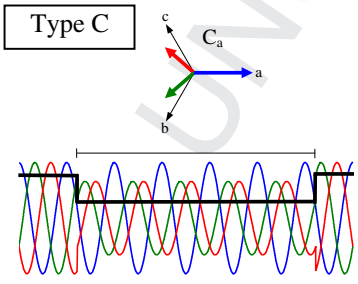 | Type $G_2$ 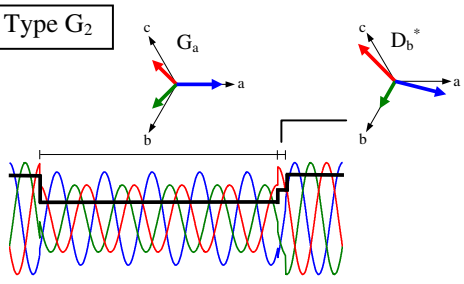 |

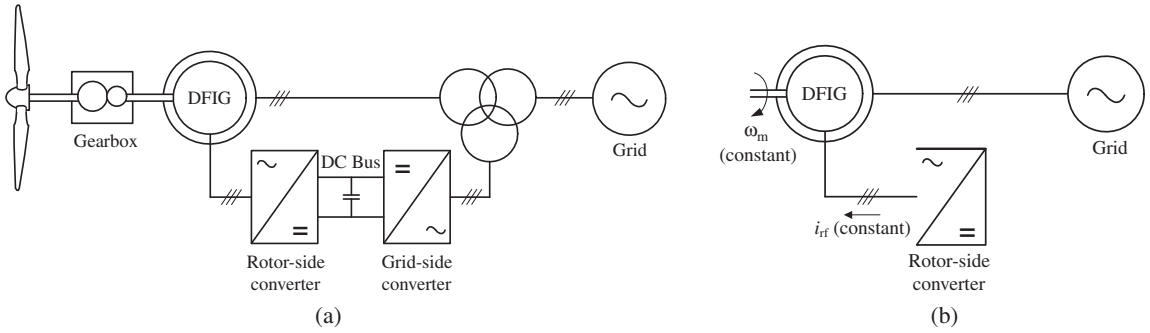


**Fig. 1.** DFIG-based WT. (a) Basic scheme in the literature; and (b) scheme with the simplifications considered in this paper.

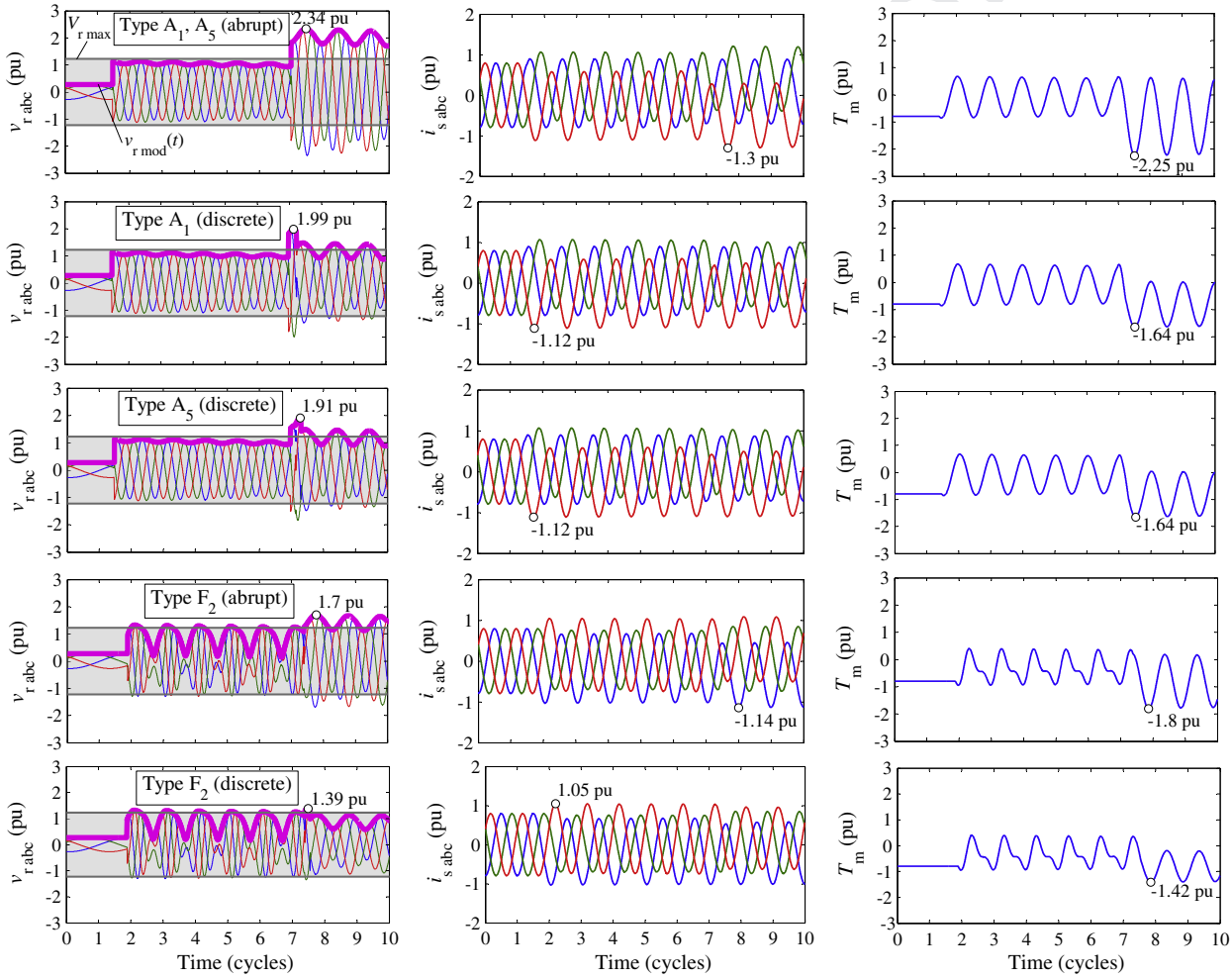


**Fig. 2.** DFIG exposed to symmetrical sag types $A_1$ and $A_5$ (modeled with abrupt and discrete recoveries) and to unsymmetrical sag type $F_2$ (modeled with abrupt and discrete recoveries). Sag characteristics: $h = 0.1$, $\Delta t = 5.5T$ and $\psi = 80°$. WT operating point 1: $P_n$ and $s = -0.27$. The shaded area corresponds to the situations where the rotor current can be controlled.

faulted behavior and a hysteresis current controller for over-current protection during system faults (this current controller maintains the pre-fault current).

(2) As sags occur during a short time interval (around 100 ms), it is also assumed that the mechanical speed cannot change significantly during the event.

According to the first assumption, by substituting $pi_{rf} = 0$ in (1), results in

$$\begin{aligned} v_{sf} &= [R_s + L_s(p + j\omega_s)]i_{sf} + j\omega_s M i_{rf} \\ v_{rf} &= (R_r + js\omega_s L_r)i_{rf} + M(p + js\omega_s)i_{sf}. \end{aligned} \quad (2)$$

The current $i_{sf}$ is obtained from the first equation of (2):

$$pi_{sf} = \frac{1}{L_s}[v_{sf} - (R_s + j\omega_s L_s)i_{sf} - j\omega_s M i_{rf}], \quad (3)$$

and by replacing (3) in the second equation of (2), we obtain

Please cite this article in press as: Rolán A et al. Detailed study of DFIG-based wind turbines to overcome the most severe grid faults. Int J Electr Power Energ Syst (2014), http://dx.doi.org/10.1016/j.ijepes.2014.05.031

$$v_{rf} = \left[R_r + j\omega_s\left(sL_r - \frac{M^2}{L_s}\right)\right] i_{rf} + M\left[-\frac{R_s}{L_s} + j\omega_s(s-1)\right] i_{sf} + \frac{M}{L_s} v_{sf}. \quad (4)$$

Fig. 1 shows the basic scheme of the DFIG-based WT in the literature (Fig. 1(a)) and the scheme considering the aforementioned two assumptions (Fig. 1(b)).

Fig. 2 shows the time evolution of the rotor voltages, $v_{r\ abc}$, stator currents, $i_{s\ abc}$, and electromagnetic torque, $T_m$, of the DFIG exposed to symmetrical and unsymmetrical sags. The studied variables are expressed in pu according to the base values $S_b$ = 2 MW, $f_b$ = 50 Hz, $U_b$ = 690 V, $I_b = S_b/(\sqrt{3}U_b) = 1673.5$ A, $T_b = S_b/(\omega_b/\wp) = 12.73$ kNm (where $\omega_b = 2\pi f_b$ and $\wp = 2$ is the number of pole pairs) as

$$v_{r\ abc\ pu}(t) = \frac{v_{r\ abc}(t)}{\sqrt{2}V_b}, \quad i_{s\ abc\ pu}(t) = \frac{i_{s\ abc}(t)}{\sqrt{2}I_b}, \quad T_{m\ pu}(t) = \frac{T_{m(t)}}{T_b}, \quad (5)$$

where $V_b = U_b/\sqrt{3} = 398.4$ V is the per-phase base voltage. For simplicity purposes, subscript pu is omitted in the remaining of the paper.

Fig. 2 also shows the time evolution of $v_{r\ mod}(t)$, defined as

$$v_{r\ mod}(t) = \sqrt{\frac{2}{3}}\sqrt{v_{ra}^2(t) + v_{rb}^2(t) + v_{rc}^2(t)}. \quad (6)$$

This variable $v_{r\ mod}(t)$, which corresponds to the well-known amplitude of the space vector of the rotor voltages [19], represents the rotor voltage required to control the transformed rotor current, $i_{rf}$, according to a desired control law. If $V_{r\ max}$ is the maximum amplitude of the fundamental per-phase voltage which can be generated by the rotor-side converter when $v_{r\ mod}(t)$ satisfies

$$v_{r\ mod}(t) \leqslant V_{r\ max}, \quad (7)$$

the rotor current can be controlled or, in the control law of this paper, the current $i_{rf}$ can be kept constant.

The value of $V_{r\ max}$ for the example of this paper is calculated as follows. $V_{r\ max}$ depends on the DC-link voltage, $V_{dc}$ (reduced to the stator), according to [4]:

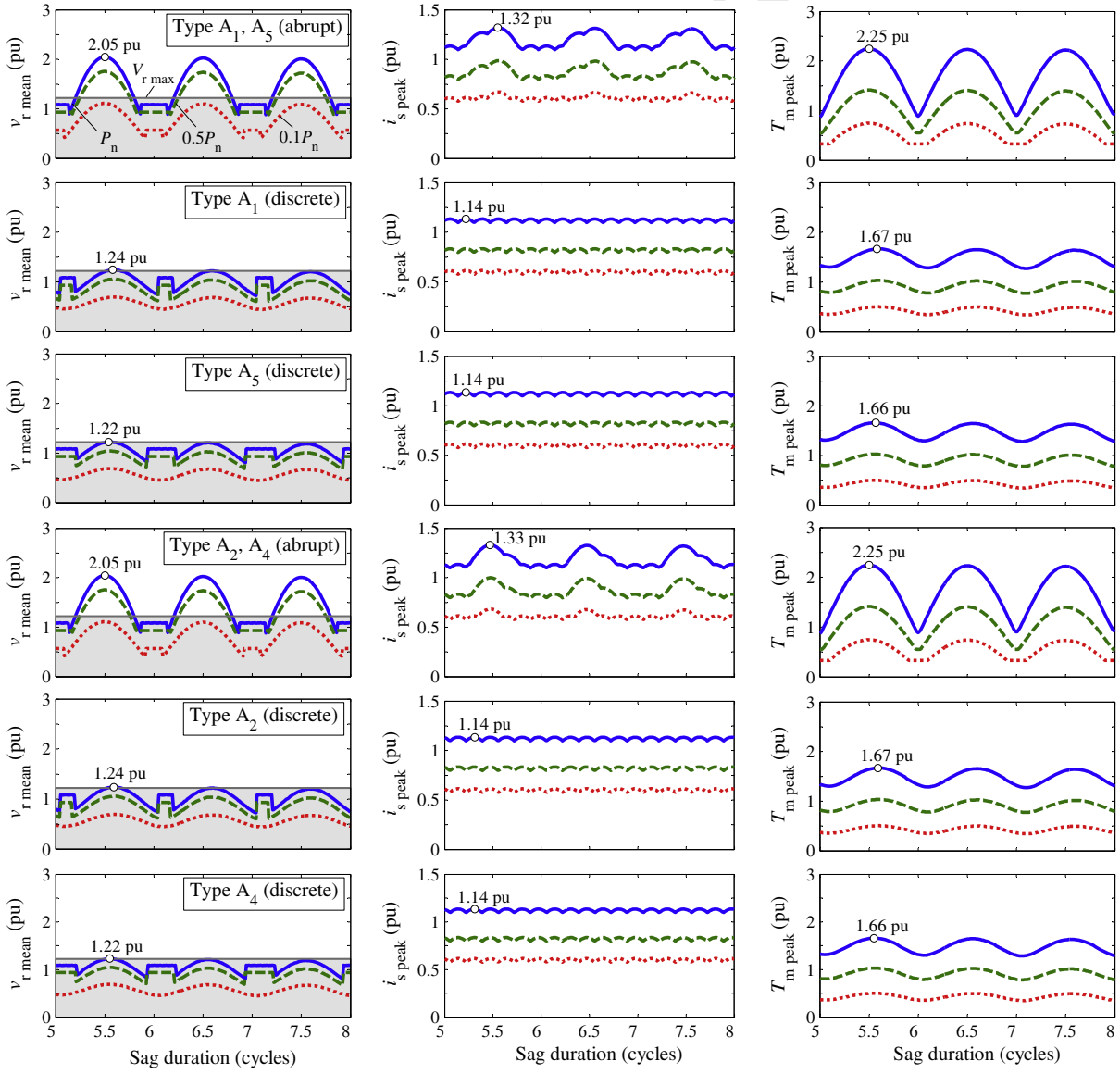


**Fig. 3.** Sag duration influence on DFIG exposed to symmetrical sags modeled with abrupt and discrete recoveries. Sag characteristics: $h$ = 0.1, $\Delta t = 5T \ldots 8T$ and $\psi = 80°$. WT operating points: 1 ($P_n$, solid line), 2 ($0.5P_n$, dashed line) and 3 ($0.1P_n$, dotted line). The shaded area corresponds to the situations where the rotor current can be controlled.

Please cite this article in press as: Rolán A et al. Detailed study of DFIG-based wind turbines to overcome the most severe grid faults. Int J Electr Power Energ Syst (2014), http://dx.doi.org/10.1016/j.ijepes.2014.05.031

$$V_{r\,max} = mV_{dc}/2, \tag{8}$$

where $m$ is the modulation index. Considering the space vector modulation technique ($m = 1.15$) and a DC-link voltage of 1200 V (reduced to the stator), a maximum amplitude of $V_{r\,max} = 690$ V (reduced to the stator) or 1.22 pu is obtained. Note that $V_{dc} = 1200$ V for a DFIG-based wind turbine with nominal values 2 MW and 690 V is high enough for the converter to become a full-converter wind generation solution.

## Sag characteristics influence

The stator current peak, $i_{s\,peak}$, and the electromagnetic torque peak, $T_{m\,peak}$, (obtained during the sag or after voltage recovery) are chosen as indicators of DFIG sensitivity to voltage sags. They are referred to the base values as

$$i_{s\,peak\,pu} = \frac{i_{s\,peak}}{\sqrt{2}I_b} = \frac{\max\{|i_{sa}(t)|, |i_{sb}(t)|, |i_{sc}(t)|\}}{\sqrt{2}I_b}$$
$$T_{m\,peak\,pu} = \frac{T_{m\,peak}}{T_b} = \frac{\max\{|T_{m(t)}|\}}{T_b}. \tag{9}$$

The required peak value of $v_{r\,mod}(t)$ in the discrete sags of Fig. 2 is larger than the rotor-side converter voltage limit, $V_{r\,max}$. However, this peak occurs only once, specifically after fault clearing (unlike the required peaks in the abrupt sags of Fig. 2, which are periodically repeated after fault clearing). Thus, this single peak can lead to the misinterpretation that the rotor current cannot be controlled. To solve this problem, a new variable is defined to quantify if the rotor current can be controlled in an averaged sense

$$v_{r\,mean} = \frac{1}{T}\int_{t_a}^{t_a+T} v_{r\,mod}(t)dt \quad \rightarrow \quad v_{r\,mean\,pu} = \frac{v_{r\,mean}}{\sqrt{2}V_b}. \tag{10}$$

The mean value of the rotor voltage, $v_{r\,mean}$, is evaluated at the first period after $v_{r\,mod}(t)$ reaches its maximum value. The instant $t_a$ in (10) is chosen as $t_a = t_{vr\,max} + T/2$ ($t_{vr\,max}$ is the instant when $v_{r\,mod}(t)$ is maximum). For example, the mean values of the rotor voltage for the symmetrical sags in Fig. 2 are: $v_{r\,mean} = 2.05$ pu (type $A_1$ and $A_5$ abrupt), $v_{r\,mean} = 1.24$ pu (type $A_1$ discrete), and $v_{r\,mean} = 1.22$ pu (type $A_5$ discrete). These values are highlighted in Fig. 3.

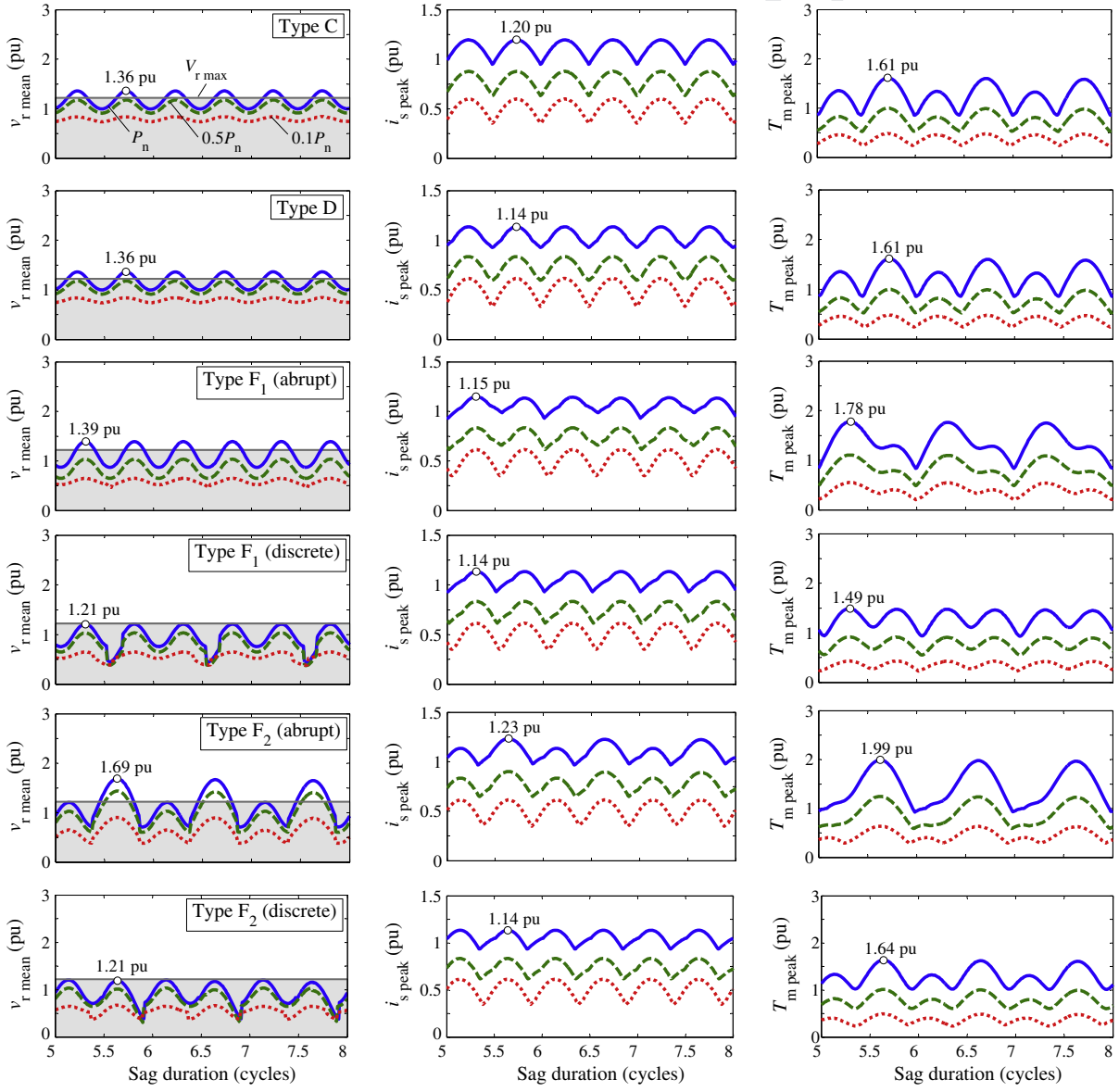


**Fig. 4.** Sag duration influence on DFIG exposed to unsymmetrical sag types C, D, $F_1$ and $F_2$ modeled with abrupt and discrete recoveries. Sag characteristics: $h = 0.1$, $\Delta t = 5T \ldots 8T$ and $\psi = 80°$. WT operating points: 1 ($P_n$, solid line), 2 ($0.5P_n$, dashed line) and 3 ($0.1P_n$, dotted line). The shaded area corresponds to the situations where the rotor current can be controlled.

Please cite this article in press as: Rolán A et al. Detailed study of DFIG-based wind turbines to overcome the most severe grid faults. Int J Electr Power Energ Syst (2014), http://dx.doi.org/10.1016/j.ijepes.2014.05.031

It is apparent that if the symmetrical sags of Fig. 2 are modeled abrupt, the predicted rotor voltage necessary to overcome these sags is 2.05 pu; that is, a converter of 2.05 times the rated stator voltage is required. However, if the same sags are modeled in a more realistic way (discrete sags), the predicted rotor voltage needed to control the rotor current is reduced to 1.22 times the rated stator voltage. Assuming that the rotor-side converter power is approximately $s$ times the DFIG rated power ($s$ is the machine electromechanical slip), it is necessary to protect the rotor-side converter properly in order to overcome the most severe sags.

It should also be noted that the most severe sags are considered in this paper; that is, sags originated at the point of common connection. Nonetheless, faults in realistic situations are originated far from the DFIG, causing less severe voltage depths at the stator terminals than those studied in this paper. Then, if the rotor-side converter is properly protected to overcome the sags in this paper, it will be able to overcome any fault occurring in realistic situations.

*Sag duration influence*

All the simulated sags in Fig. 2 have the same duration ($\Delta t = 5.5T$). An exhaustive study including the range of sag duration values $5T \leqslant \Delta t \leqslant 8T$ is presented in this section. The sag duration influence on $v_{r\,mean}$, $i_{s\,peak}$ and $T_{m\,peak}$ is illustrated for the symmetrical sags, Fig. 3, and for the unsymmetrical sags, Figs. 4 and 5. The three WT operating points in Section 'DFIG-based WT characteristics' are considered. The following observations can be made from the figure results:

(1) The effect of both abrupt and discrete sags on the variables of interest is periodical, as the values of these variables are repeated each cycle. Table 2 summarizes the most unfavorable sag durations for all sag types, defined as the durations causing the largest peaks on the DFIG variables, according to Figs. 3–5. The most unfavorable sag durations are periodical because the effects on the DFIG variables are also periodical.
(2) If sags are modeled discrete the peaks of the variables predicted are smaller than if sags are modeled abrupt. Thus, (the more realistic) discrete sags predict less severe consequences than (the less realistic) abrupt sags.
(3) The discrete sag types $A_4$ and $A_5$ (sags with three-step voltage recovery) are less severe than the discrete sag types $A_1$ and $A_2$ (sags with two-step voltage recovery). This shows that the increase in the number of steps during voltage recovery smoothes sag effects.
(4) When sags are modeled abrupt, the rotor voltage predicted is $v_{r\,mean} > V_{r\,max}$; that is, they predict that the rotor current cannot be controlled. However, the more realistic discrete sags predict that the rotor voltage is $v_{r\,mean} < V_{r\,max}$; that is, they predict that the rotor current can be controlled.
(5) Regarding the WT operating points, the largest peaks in all variables occur when the DFIG delivers its rated power, $P_n$, to the electrical grid. In contrast, the smallest peaks occur when the power delivered is $0.1P_n$. Thus, the WT operating point 1 is the most unfavorable.
(6) Unsymmetrical sags are less severe than symmetrical sags as the peaks in all variables studied are smaller.

From these results it is apparent that the effects of the following pairs of sag types are similar: $A_1$ and $A_2$ (abrupt), $A_1$ and $A_2$ (discrete), $A_4$ and $A_5$ (discrete), C and D, $F_1$ and $G_1$ (abrupt), $F_1$ and $G_1$ (discrete), $F_2$ and $G_2$ (abrupt) and $F_2$ and $G_2$ (discrete).

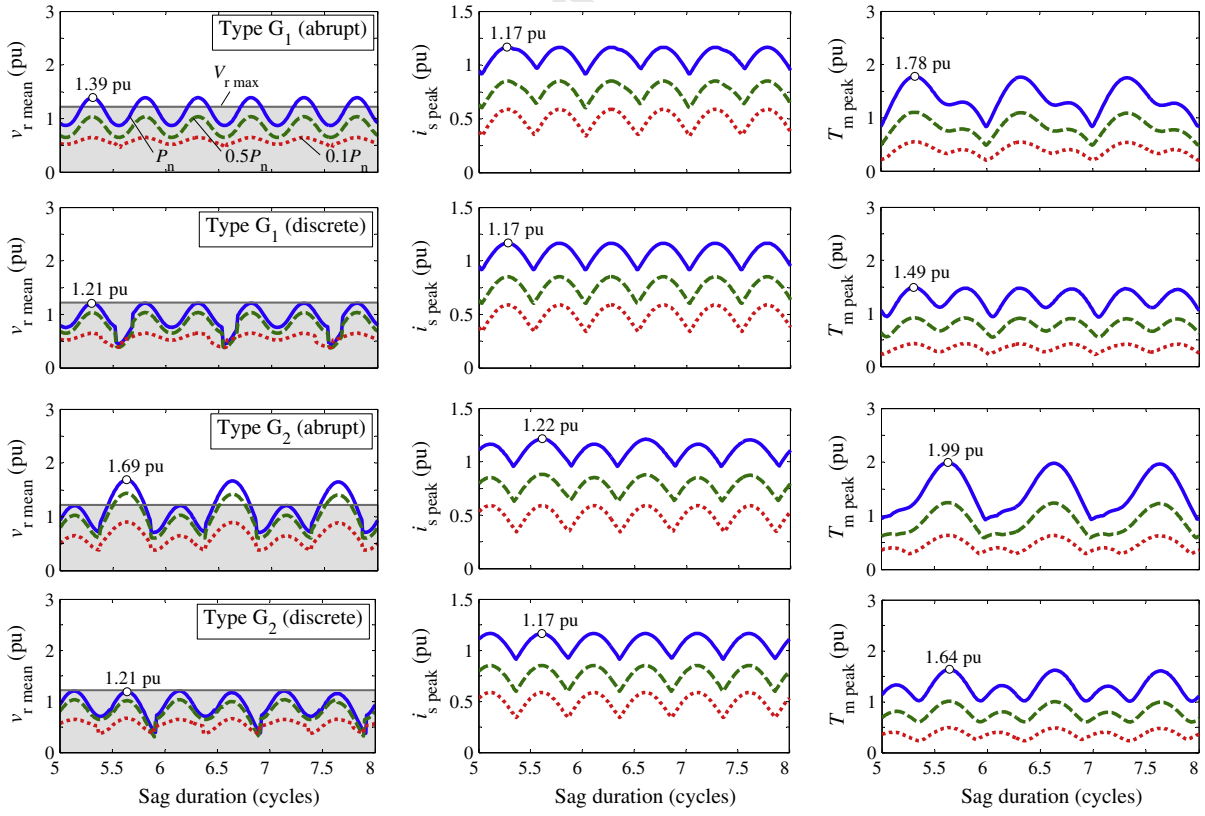


**Fig. 5.** Sag duration influence on DFIG exposed to unsymmetrical sag types $G_1$ and $G_2$ modeled with abrupt and discrete recoveries. Sag characteristics: $h = 0.1$, $\Delta t = 5T \ldots 8T$ and $\psi = 80°$. WT operating points: 1 ($P_n$, solid line), 2 ($0.5P_n$, dashed line) and 3 ($0.1P_n$, dotted line). The shaded area corresponds to the situations where the rotor current can be controlled.

Please cite this article in press as: Rolán A et al. Detailed study of DFIG-based wind turbines to overcome the most severe grid faults. Int J Electr Power Energ Syst (2014), http://dx.doi.org/10.1016/j.ijepes.2014.05.031

**Table 2**
Most unfavorable durations for each sag type and sag depths from which the rotor current can be controlled (if rotor voltage equals stator voltage).

| Type | Model | Most unfavorable duration ($n = 0, 1, 2\ldots$) | Sag depth |
|---|---|---|---|
| $A_1$ and $A_2$ | Abrupt | $\Delta t = nT + T/2$ | $h \geqslant 0.45$ |
| $A_1$ and $A_2$ | Discrete | $\Delta t = nT + 0.7T$ | $h \geqslant 0.05$ |
| $A_4$ and $A_5$ | Abrupt | $\Delta t = nT + T/2$ | $h \geqslant 0.45$ |
| $A_4$ and $A_5$ | Discrete | $\Delta t = nT + 0.6T$ | $h \geqslant 0.05$ |
| C and D | Abrupt or discrete | $\Delta t = nT + 0.7T$ | $h \geqslant 0.2$ |
| $F_1$ and $G_1$ | Abrupt | $\Delta t = nT + 0.3T$ | $h \geqslant 0.2$ |
| $F_1$ and $G_1$ | Discrete | $\Delta t = nT + 0.3T$ | $h \geqslant 0.05$ |
| $F_2$ and $G_2$ | Abrupt | $\Delta t = nT + 0.6T$ | $h \geqslant 0.35$ |
| $F_2$ and $G_2$ | Discrete | $\Delta t = nT + 0.6T$ | $h \geqslant 0.05$ |

*Sag depth influence*

The mean rotor voltage, $v_{r\,mean}$, is chosen as the variable to study the sag depth influence on the DFIG. In the previous subsections, it is proved that this variable is very important when studying the DFIG behavior under voltage sags because it defines the situations where the rotor current can be controlled. The 3D graphics in Fig. 6 illustrate the influence of sag depth, $h$, and power generated, $P$, on the mean rotor voltage for all sag types. In order to illustrate the situations where the rotor current can be controlled, sag depth and power generated take all possible values ($0 \leqslant h \leqslant 1$ and $0 \leqslant P \leqslant P_n$), and the most unfavorable duration for each sag type is considered (see Table 2). The 3D graphs also contain the $V_{r\,max}$ plane: the rotor current can be controlled in the regions where the $v_{r\,mean}$ plane is located under the $V_{r\,max}$ plane. The minimum sag depths for the effective control of the rotor current (based on the regions of the $v_{r\,mean}$ plane located under the $V_{r\,max}$ plane in Fig. 6) are given in Table 2 as a summary.

The results in Fig. 6 show that:

(1) Discrete sags are less severe than abrupt ones as the $v_{r\,mean}$ planes are always in a lower position than those corresponding to the abrupt case. What is more, if sags are modeled with the more realistic discrete recovery, the model predicts that the rotor current can be controlled for almost all sag depths as almost all regions of the $v_{r\,mean}$ plane are located under the $V_{r\,max}$ plane.
(2) Unsymmetrical sags are less severe than symmetrical ones because the $v_{r\,mean}$ planes are located in a lower position than those corresponding to symmetrical sags.
(3) There is a similarity between the effects caused by the following sag types: $A_1$ and $A_2$ (abrupt and discrete), $A_4$ and $A_5$ (abrupt and discrete), C and D, $F_1$ and $G_1$ (abrupt and discrete), and $F_2$ and $G_2$ (abrupt and discrete). Note that the same observation was made for the sag duration influence.
(4) In view of the above effects, sags could now be classified into three typologies only:
  - Symmetrical sags (types $A_1$, $A_2$, $A_4$ and $A_5$).
  - Unsymmetrical sags due to 1-phase-to-ground or 2-phase faults (types C and D).
  - Unsymmetrical sags due to 2-phase-to-ground faults (types $F_2$ and $G_2$, as they are more severe than $F_1$ and $G_1$).

*The most severe grid faults*

Table 2 summarizes the most severe grid faults which can be overcome by the rotor-side converter. As specified in Section 'Sag duration influence', the table shows the most unfavorable sag durations for all sag types, according to Figs. 3–5. These most unfavorable durations correspond to the control strategy considered (constant rotor current in the synchronous reference frame); the use of other control strategies may result in different unfavorable durations.

As described in section 'Sag depth influence', Table 2 also includes the minimum sag depths for the effective control of the rotor current (based on the regions of the $v_{r\,mean}$ plane located under the $V_{r\,max}$ plane in Fig. 6). Note that the discrete sag model predicts that the rotor current can be controlled for almost all sag depths.

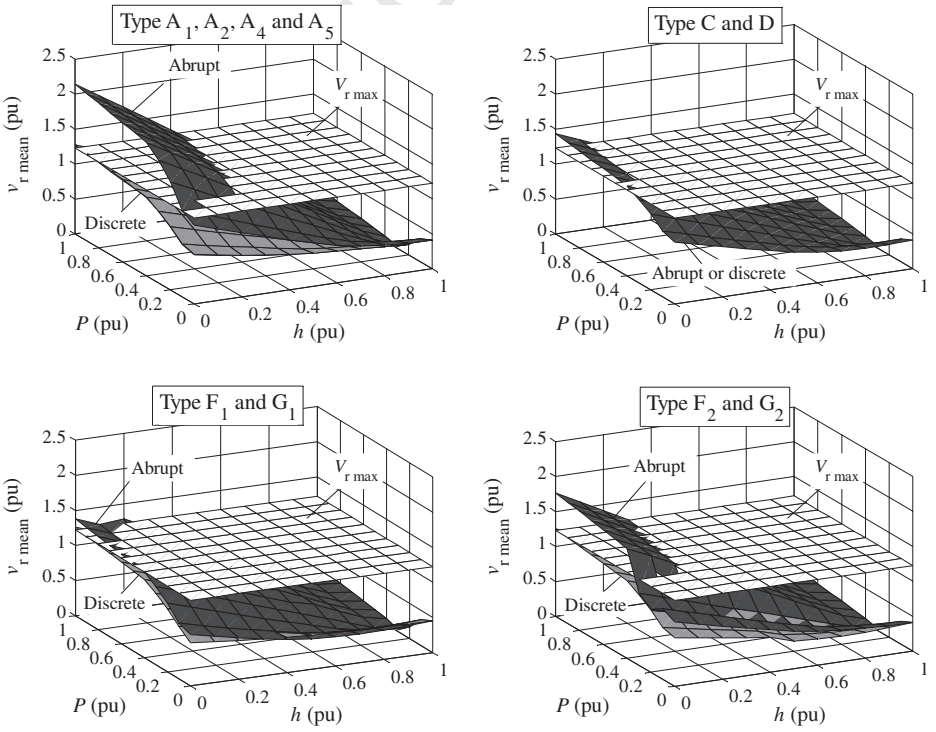


**Fig. 6.** Sag depth influence on the mean rotor voltage of DFIG exposed to voltage sags considering all possible values of power generated. Sag characteristics: $h = 0\ldots1$, $\Delta t$ is the most unfavorable duration for each sag type and $\psi = 80°$. The rotor current can be controlled in the regions of the $v_{r\,mean}$ plane located under the $V_{r\,max}$ plane.

Please cite this article in press as: Rolán A et al. Detailed study of DFIG-based wind turbines to overcome the most severe grid faults. Int J Electr Power Energ Syst (2014), http://dx.doi.org/10.1016/j.ijepes.2014.05.031

*Comments about the proposed control strategy*

The proposed control strategy protects the rotor converter from the large current peaks. The assumption of constant rotor current is a good way to properly control the power converter when the voltage sag starts and during voltage recovery, as there will appear no rotor current peaks during the entire event.

According to [20], we can state that the proposed control is valid (in fact it is suitable) for Period 1 (very few cycles after the voltage sag starts) and for Period 3 (voltage recovery). Moreover, considering that most of voltage sag durations are around 100 ms (short-time durations), the presented approach is good enough to provide fault ride-through to DFIG-based WTs [6]. During the fault event (Period 2) the authors recognize that the

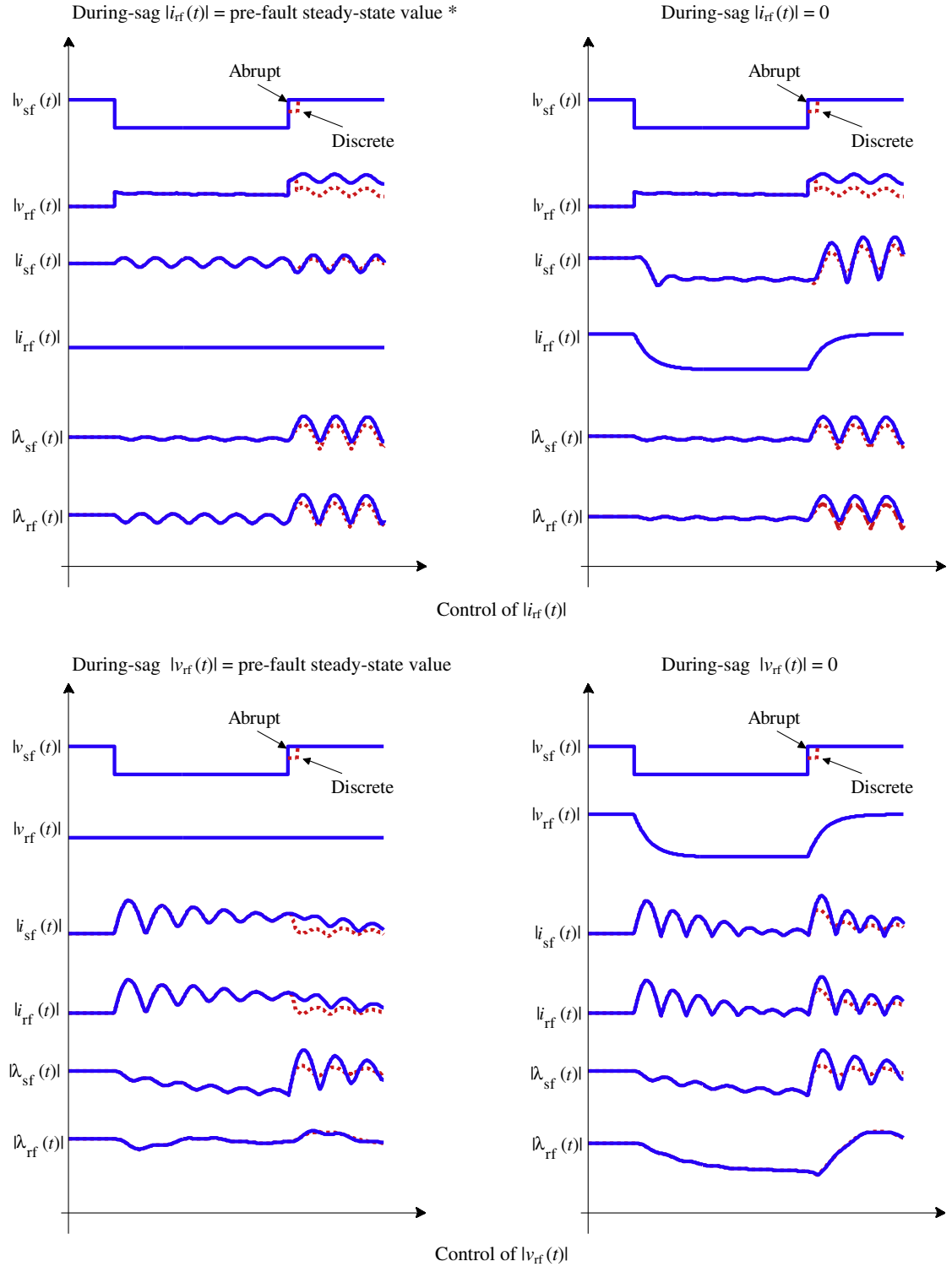


**Fig. 7.** Types of DFIG control: control of $|i_{rf}|$ and control of $|v_{rf}|$. Sag characteristics: $h = 0.1$, $\Delta t = 5.5T$ and $\psi = 80°$.

Please cite this article in press as: Rolán A et al. Detailed study of DFIG-based wind turbines to overcome the most severe grid faults. Int J Electr Power Energ Syst (2014), http://dx.doi.org/10.1016/j.ijepes.2014.05.031

proposed control is not an optimal control. Certainly, although this control strategy also maintains DFIG controllability as established in current grid codes (i.e., providing reactive current during the fault) it is not as robust as other controls in the literature (such as [13–16]). However, the proposed control has an important advantage: it allows the electrical transient to be solved analytically, providing and an excellent tool for the comprehension of DFIG dynamic behavior subject to voltage sags (the detailed analytical model is shown in [5]).

As the proposed control is analytical, it allows a large number of scenarios to be easily studied. The current author's work is a continuation of the previous work [5] because now DFIG under voltage sags is exhaustively studied considering a large number of sag durations and depths, which helps in the fault ride-through for different fault scenarios.

It is apparent that a constant rotor current results in a high rotor voltage (as shown in previous sections, the required rotor voltage for the most unfavorable sag durations and depths is higher than the converter voltage limit). Other smoothing strategies would require lower rotor voltages at the expense of increasing current peaks.

Let's consider the control strategies commented in Section 'DFIG control strategies during voltage sags': Fig. 7 shows the time evolution of the DFIG variables when controlling the transformed rotor current, $|i_{rf}|$, and when controlling the transformed rotor voltage, $|v_{rf}|$, considering two cases: when the during-sag controlled variable equals its pre-fault steady-state value (left side of Fig. 7) and when it is reduced to 0 (right side of Fig. 7). It is observed that the rotor voltage noticeably changes if the rotor current is kept constant (top left of Fig. 7). Inversely, the rotor current clearly varies if the rotor voltage is kept constant (bottom left of Fig. 7). Naturally, if a variation in the rotor current is allowed in the control (top right of Fig. 7), the during-sag rotor voltage peaks will decrease. Conversely, if a variation in the rotor voltage is allowed in the control (bottom right of Fig. 7), smaller rotor current peaks will be produced during the sag.

Regarding the stator and rotor fluxes, $\lambda_{sf}$ and $\lambda_{rf}$, respectively, the way to reduce them during the sag is by means of controlling the rotor voltage. However, note that after voltage recovery there appear large peaks in all the variables. Another way to properly reduce the stator rotor fluxes would be the use of a crowbar, as shown in Fig. 8. Note that as it happens with the control of the transformed rotor voltage, although the fluxes are reduced during the sag, after voltage recovery there appear large peaks. It should also be noted that these peaks are reduced when considering the discrete model for the sag, which is one of the main contributions of the paper.

All of this leads to the following conclusions:

(1) Certainly, although the proposed control strategy does not reduce the stator and rotor fluxes during the fault (top left of Fig. 7), the behavior of the machine after voltage recovery is not worse than in the other cases: note that when the sag ends, there appear peaks in all the variables, independently of the adopted control strategy.
(2) The peaks that appear after voltage recovery are reduced if the voltage sag is modeled discrete. In other words, the more realistic approach for sag modeling (discrete sag modeling) is less restrictive when analyzing the machine's behavior under such grid disturbances.

Lastly, it should be noted that with the proposed control strategy, unsymmetrical sags are less severe than symmetrical sags. However, the different severities of the balanced and unbalanced voltage sags are due to the control philosophy adopted during the event, which depends on the goal to be achieved, leading to different DFIG behaviors.

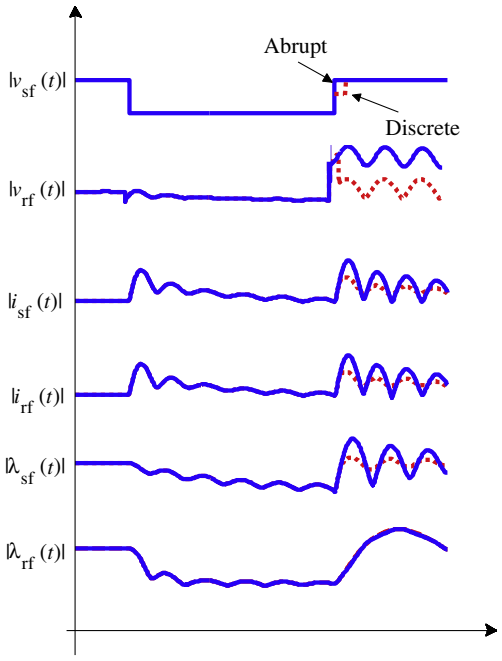


**Fig. 8.** Crowbar influence on the DFIG variables. Sag characteristics: $h = 0.1$, $\Delta t = 5.5T$ and $\psi = 80°$.

## Conclusions

The effects of symmetrical and unsymmetrical sags on DFIGs are studied under the assumption that the rotor-side converter can keep constant the transformed rotor current in the synchronous reference frame. The proposed control protects the rotor converter from the large current peaks and maintains the DFIG controllability as established in many transmission system operator grid codes; i.e. not only to stay connected during the fault, but also to contribute to the system stability during and after the fault clearance by means of the active and reactive current during and after the event. The voltage limit of the rotor-side converter is considered in the discussion on whether the rotor current can be effectively controlled. The study helps in the understanding of WT fault ride-through capability.

The simplification made in this study is very useful because some interesting conclusions can be easily drawn: the situations where the rotor current cannot be controlled correspond to rotor voltage values larger than the voltage limit of the rotor-side converter (assuming that rotor voltage equals stator voltage).

The results reveal that the sag duration influence on stator current, rotor voltage and torque peaks is periodical as these peaks are repeated every cycle. These peaks appear at the here-defined most unfavorable sag duration, which is different for each sag type. This duration is used to study the sag depth influence on the rotor voltage required to control the rotor current. It is observed that there is a sag depth from which this current cannot be controlled. This limit is less restrictive in unsymmetrical sags as these are less severe than symmetrical ones.

Sag modeling and its influence on DFIG behavior are also discussed. The results show that (the more realistic) discrete recovery sags are less severe than abrupt recovery sags (the most usual approach in the literature) because the successive voltage recovery steps in the fault-clearing process smooth the effects. What is more, it is observed that the rotor current can be controlled for almost all sag depth if voltage sags are modeled with discrete recovery. Thus, abrupt recovery sags overestimate sag severity.



Please cite this article in press as: Rolán A et al. Detailed study of DFIG-based wind turbines to overcome the most severe grid faults. Int J Electr Power Energ Syst (2014), http://dx.doi.org/10.1016/j.ijepes.2014.05.031

This paper provides a very useful table (Table 2) and a 3D figure (Fig. 6) which summarizes the most severe effects on the rotor-side converter of DFIG-based WTs: most unfavorable sag durations and minimum sag depths from which the rotor current can be controlled.

Resemblances between the effects caused by the following pairs of sag types are found: $A_1$–$A_2$ (abrupt and discrete), $A_4$–$A_5$ (discrete), C–D, $F_1$–$G_1$ (abrupt and discrete), and $F_2$–$G_2$ (abrupt and discrete). Therefore, when studying sag effects on DFIGs, it is enough to consider only one sag type of each group.

In conclusion, the analysis of other controls for the DFIG rotor current should consider the possible duration periodicity effect and most unfavorable duration for each sag type, as well as a discrete sag model.

## Acknowledgements

The authors acknowledge the financial support of the Spanish Ministry of Economy and Competitiveness through Project DPI2011-28021.

## References

[1] Ackermann T. Wind power in power systems. Chichester: John Wiley & Sons; 2005.
[2] European Wind Energy Association, Wind energy – The facts. Part I: Technology, Technical Report; 2009. <http://www.ewea.org/>.
[3] Chondrogiannis S, Barnes M. Specification of rotor side voltage source inverter of a doubly-fed induction generator for achieving ride-through capability. IET Renewable Power Generation 2008;2(3):139–50.
[4] Hu J, He Y. DFIG wind generation systems operating with limited converter rating considered under unbalanced network conditions – analysis and control design. Renewable Energy 2011;36(2):829–47.
[5] Rolán A, Córcoles F, Pedra J. Doubly fed induction generator subject to symmetrical voltage sags. IEEE Trans Energy Convers 2011;26(4):1219–29.
[6] Bollen MHJ. Understanding power quality problems: voltage sags and interruptions. New York: IEEE Press; 2000.
[7] Bollen MHJ. Voltage recovery after unbalanced and balanced voltage dips in three-phase systems. IEEE Trans Power Delivery 2003;18(4):1376–81.
[8] Ku YH. Transient analysis of AC machinery. AIEE Trans 1929;48:707–14.
[9] Ling Y, Cai X. Rotor current dynamics of double fed induction generators during grid voltage dip and rise. Int J Electr Power Energy Syst 2013;44:17–24.
[10] Jadhav HT, Roy R. A comprehensive review on the grid integration of doubly fed induction generator. Int J Electr Power Energy Syst 2013;49:8–18.
[11] Amuthan N, Subburaj P, Melba Mary P. Direct model reference adaptive internal model controller for better voltage sag ride through in doubly fed induction generator wind farms. Int J Electr Power Energy Syst 2013;47:255–63.
[12] Kassem AM, Hasaneen KM, Yousef AM. Dynamic modeling and robust power control of DFIG driven by wind turbine at infinite grid. Int J Electr Power Energy Syst 2013;44:375–82.
[13] Xiang D, Ran L, Tavner PJ, Yang S. Control of a doubly fed induction generator in a wind turbine during grid fault ride-through. IEEE Trans Energy Convers 2006;21(3):652–62.
[14] Lima FKA, Luna A, Rodríguez P, Watanabe EH, Blaabjerg F. Rotor voltage dynamics in the doubly fed induction generator during grid faults. IEEE Trans Power Electron 2010;25(1):118–30.
[15] Mohseni M, Islam SM, Masoum MAS. Impacts of symmetrical and asymmetrical voltage sags on DFIG-based wind turbines considering phase-angle jump, voltage recovery and sag parameters. IEEE Trans Power Electron 2011;26(5):1587–98.
[16] Mohseni M, Islam SM, Masoum MAS. Fault ride-through capability enhancement of doubly-fed induction wind generators. IET Renewable Power Generation 2011;5(5):368–76.
[17] Zhang Z, Xu L, Zhang Y, Guan B. Novel rotor-side control scheme for doubly fed induction generator to ride through grid faults. In: Proceedings of the IEEE energy conversion congress and exposition, ECCE'10, Atlanta, USA; September 12–16, 2010. P. 3084–90.
[18] Zhang L, Jin X, Ma T, Tong Y. An improved control scheme for doubly fed induction generator during grid fault ride-through. In: Proceedings of the 3rd IEEE international symposium on power electronics for distributed generation systems, PEDG'12, Aalborg, Denmark; June 25–28, 2012. p. 301–6.
[19] Vas P. Electrical machines and drives – a space-vector theory approach. New York: Oxford University Press; 1996.
[20] Geng H, Liu C, Yang G. LVRT capability of DFIG-based WECS under asymmetrical grid fault condition. IEEE Trans Ind Electron 2013;60(6):2495–509.